Smart Materials in Medicine 2 (2021) 292–301

Contents lists available at ScienceDirect

Smart Materials in Medicine

journal homepage: www.keaipublishing.com/en/journals/smart-materials-in-medicine/

Biocompatible composite films and fibers based on Poly(Vinyl alcohol) and powders of calcium salts

K. Kh Peranidze [a,*], T.V. Safronova [a], N.R. Kil'deeva [b], M.V. Chernogortseva [b], I.I. Selezneva [c], T.B. Shatalova [a], J.V. Rau [d,e]

[a] Lomonosov Moscow State University, Leninskie Gory 1, 119991, Moscow, Russian Federation
[b] Kosygin Russian State University, Malaya Kaluzhskaya 1, 119071, Moscow, Russian Federation
[c] Institute of Theoretical and Experimental Biophysics, Russian Academy of Sciences, 142292, Pushchino, Russian Federation
[d] Istituto di Struttura Della Materia, Consiglio Nazionale Delle Ricerche (ISM-CNR), Via Del Fosso Del Cavaliere 100, 00133, Rome, Italy
[e] Sechenov First Moscow State Medical University, Trubetskaya 8, Build. 2, 119991, Moscow, Russian Federation

ARTICLE INFO

Keywords:
poly(vinyl alcohol) hydrogels
Brushite
Hydroxyapatite
Calcium carbonate
Electrospinning
Dental pulp stem cells

ABSTRACT

A method for obtaining composite biodegradable materials in the form of films and fibers, based on hydrophilic poly(vinyl alcohol) matrix and synthetic nanopowders of calcium salts containing phosphate and/or carbonate anions, was proposed. The phase composition of fillers previously synthesized from $Ca(CH_3COO)_2{\cdot}H_2O$, $(NH_4)_2HPO_4$ and/or $(NH_4)_2CO_3$ aqueous solutions at a chosen ratio of components was represented by hydroxyapatite ($Ca_{10}(PO_4)_6(OH)_2$), brushite ($CaHPO_4{\cdot}2H_2O$), as well as calcite and vaterite polymorphs ($CaCO_3$), all of which are known to be compatible with biological cells. Filled poly(vinyl alcohol)-based nanofibers with the wide thickness range of approximately 190–530 nm were manufactured from composite suspensions by bottom-up type of electrospinning. The addition of calcium carbonate to the suspension with a particle filling degree of 20% showed a significant reduction in operating voltages (from 42 kV to 28 kV) during electrospinning process and, as a result, facilitated stable fiber formation. According to the microscopy data, the average size of inorganic inclusions did not exceed 5 μm for fibrous materials, while the particle size of calcium phosphate fillers in films obtained by casting into polystyrene molds, was characterized by larger values (up to 40 μm) due to intensive crystallization process on film surfaces. The biocompatible phase composition and structural features, including surface roughness and special particle morphology, ensures a potential application of the studied materials as filled scaffolds for the multipotent stromal cells cultivation in bone tissue engineering.

1. Introduction

Over the past few years, bioscaffolding has become one of the main trends in bone tissue engineering. According to this technique, the issues of bone defects elimination can be solved by developing individual biocompatible biodegradable materials based on three-dimensional porous or fibrous polymer matrices (scaffolds) [1], which are populated with donor multipotent mesenchymal stromal cells differentiating into osteoblasts under certain environmental conditions within the material [2]. In order to ensure and maintain osteogenic cell differentiation, bioscaffolding involves the embedding of various osteogenesis inducers (dexamethasone [3], β-glycerophosphate [4], bioresorbable inorganic phosphates [5], specific bone morphogenetic proteins [6], etc.) into the cultivation system that reveals the ways of using the investigated materials as drug carriers.

The crucial task of modern materials science is related to the development of new-generation composite materials made of biocompatible synthetic polymers and calcium phosphates [7,8] intended for use in combination with donor cells. A regenerative approach in tissue engineering, according to which calcium phosphate particles incorporated to polymer hydrogels act as bioactive additives promoting the cell proliferation, is considered the most appropriate today. A number of characteristics that potential scaffolds should possess includes biocompatible chemical composition, surface relief comfortable for cell differentiation and liquid-permeable architecture assuring sufficient mechanical strength and flexibility. The currently existing materials for specified

* Corresponding author.
E-mail addresses: perika5@mail.ru (K.K. Peranidze), t3470641@yandex.ru (T.V. Safronova), kildeeva@mail.ru (N.R. Kil'deeva), novissime@mail.ru (M.V. Chernogortseva), selezneva_i@mail.ru (I.I. Selezneva), shatalovatb@gmail.com (T.B. Shatalova), giulietta.rau@ism.cnr.it (J.V. Rau).

https://doi.org/10.1016/j.smaim.2021.08.002
Received 31 October 2020; Received in revised form 5 August 2021; Accepted 6 August 2021
Available online 10 August 2021

medical purposes, as well as the technologies of their manufacturing, remain far from the required parameters, and hence they cannot be fully recommended for cell cultivation with subsequent implantation into human body.

Among a great variety of natural (collagen, chitosan, fibroin, etc.) [9] and synthetic (poly(lactide), poly(glycolide), ε-poly(caprolactone), etc.) polymers [10–12], which could be used to build hydrophilic matrix serving as a mechanical frame for cells, poly(vinyl alcohol) attracts more research interest due to its high biocompatibility and gel structure forming capability in the absence of toxic reagents. The striking examples of widespread poly(vinyl alcohol) application in biomedical engineering include low-molecular (~60000–75000 Da) polymer hydrogels as materials for vascular grafting [13], poly(vinyl alcohol)-based embolization agents, as well as poly(vinyl alcohol)-based fibers, easily formed due to thermoplastic properties of the polymer, for use in surgical threads manufacturing [14]. Special attention should be paid to the membranous polymer coatings with antimicrobial activity made up of poly(vinyl alcohol) and chitosan complex hydrogels for the treatment of burns and surgical wounds [15,16]. Moreover, specified complex hydrogels are widely studied as promising drug delivery systems with controlled release [17].

Recent studies of filled polymer scaffolds for bone tissue engineering consider various calcium phosphate fillers, with the predominance of hydroxyapatite [18] or a mixture hydroxyapatite/calcium orthophosphate ($Ca_3(PO_4)_2$) [19]. In general, biocompatible calcium phosphates with a Ca/P molar ratio in the range of 0.5–1.67 have been proposed [20,21]. The selection of the desirable calcium phosphate as a bioactive filler is strictly connected with its ability to dissolve (degrade) in slightly acidic and neutral environments. Thus, the biodegradability enhances with the decrease of the Ca/P molar ratio, which can be explained in terms of thermodynamics by the rising condensation degree of the phosphate anion that leads to lower electrostatic component of the crystal lattice energy and improved hydration entropy.

The use of synthetic hydroxyapatite in biomimetic regenerative approaches is justified by its highest affinity to mineral constituent of natural bone tissue. As is known, the structure of this compound is often characterized by numerous cationic and anionic substitutions that results in variable composition [22]. Carbonate anion was shown to be one of the main sources of the hydroxyapatite lattice deformation. In particular, CO_3^{2-}-groups in B-position increase the resorption of the material, that is, they influence on the dissolution-precipitation processes in the presence of extracellular body fluids [23]. Moreover, CO_3^{2-}-groups play an important role in the biochemical interactions between bone tissue and blood plasma [24]. In a number of studies on bioceramics for bone implants, the observation of powders containing phosphate and carbonate anions is presented [25,26]. According to the studies, the addition of $CaCO_3$ to the system was carried out mainly in order to regulate the resorption rate and improve the mechanical properties of nanopowders. Therefore, from the literature analysis devoted to the development of new materials for bone tissue recovery, it follows that nano- and microscale powders in the calcium phosphate – calcium carbonate system have a great potential for mentioned medical application as bioactive fillers. Since the issues of technology and the impact of filler composition and microstructure on hybrid material properties have not been sufficiently studied, the research in this significant area of bioscaffolding remains relevant.

Currently, there exists a large number of techniques for obtaining filled polymer matrices of the desired shape, size and composition [27]. These techniques of scaffold fabrication are usually divided into two groups. The first group is based on using solvents and high temperatures and includes such methods, as electrospinning, phase separation, lyophilization and leaching, to form fibrous or porous polymer constructions [28–30]. The second group of techniques is related to rapid prototyping technologies including laser stereolithography and most frequently used 3D printing [31,32]. In the framework of this research, we focused mainly on electrospinning method of composite fibers formation in order to study fundamentally new opportunities for obtaining non-woven materials.

Thus, the present research paper is aimed at studying novel composite materials consisting of poly(vinyl alcohol)-based matrices and pre-synthesized nano- and microscale inorganic fillers, obtained in the form of films and fibers by using interdisciplinary combination of the approaches to the bioactive fillers fine inorganic synthesis and polymer hydrogels manufacturing.

2. Materials and methods

2.1. Synthesis of powder fillers

Inorganic fillers in the calcium phosphate – calcium carbonate system were synthesized from aqueous solutions of the precursors by a method we proposed in Ref. [33].

The initial components for the synthesis of $CaCO_3$ powder (CC-filler) were 1 M solutions of calcium acetate hydrate $Ca(CH_3COO)_2{\cdot}H_2O$ (Sigma Aldrich) and ammonium carbonate $(NH_4)_2CO_3$. The chemical reaction occurs in accordance with the equation (1).

$$Ca(CH_3COO)_2 + (NH_4)_2CO_3 = CaCO_3\downarrow + 2CH_3COONH_4 \quad (1)$$

A powder containing hydroxyapatite $Ca_{10}(PO_4)_6(OH)_2$ and brushite $CaHPO_4{\cdot}2H_2O$ phases (CP-filler) was obtained from 1 M solution of $Ca(CH_3COO)_2{\cdot}H_2O$ and 0.6 M solution of ammonium hydrophosphate $(NH_4)_2HPO_4$ (Sigma Aldrich) so that the theoretical Ca/P molar ratio was 1.67, which corresponded to the hydroxyapatite. As it has been shown in Ref. [33], the lack of additional pH control in the presence of CH_3COOH/CH_3COO^- buffer system formed due to the selected reagents, leads to the slightly acidic solution medium (pH ~ 4.7–6.0), and hence to the formation of $CaHPO_4{\cdot}2H_2O$ under these conditions. Thus, the reaction can be reflected by the equations (2) and (3).

$$10Ca(CH_3COO)_2 + 6(NH_4)_2HPO_4 + 2H_2O = Ca_{10}(PO_4)_6(OH)_2\downarrow + 20CH_3COONH_4 \quad (2)$$

$$Ca(CH_3COO)_2 + (NH_4)_2HPO_4 + 2H_2O = CaHPO_4{\cdot}2H_2O\downarrow + 2CH_3COONH_4 \quad (3)$$

The precipitation of the powder product containing HPO_4^{2-}- and CO_3^{2-}-anions (CC/CP-filler) from aqueous mixed-anionic solution was carried out on the basis of 1 M $Ca(CH_3COO)_2{\cdot}H_2O$ solution and 0.3 M solutions of $(NH_4)_2HPO_4$ and $(NH_4)_2CO_3$. The chemical processes, which took place during complex powder formation, are assumed to be represented by summarizing the equation (1) – (3).

After drying in a thin layer, each of the precipitated samples was placed in special container together with calculated mass of grinding ZrO_2-spheres (m_{powder}: $m_{spheres}$ = 1 : 5) and then grinded in a planetary ball mill under acetone for 20 min with subsequent evaporation of the acetone and sieving through a polyester sieve with a mesh size of 200 μm.

2.2. Preparation of composite hydrogels

Since the process of polymer fibers manufacturing was limited by the characteristics of forming solutions, the initial stage of the work was related to the selection of poly(vinyl alcohol) with suitable forming ability. In the framework of the present study, the solutions of synthetic poly(vinyl alcohol) (LLC "TITAN", 88% hydrolysis degree) of various molecular weights were tested for viscosity values and fiber forming ability by viscometry and electrospinning methods, respectively.

To prepare aqueous solutions with polymer mass fraction of 8%, the calculated amounts of poly(vinyl alcohol) were dosed into water at a room temperature and then dissolved for 6 h by stirring and heating at 75–80 °C. The calculated masses of pre-synthesized CC-, CP- and CC/CP-fillers were added to the solutions while stirring and maintaining the temperature for ~1 h until the components of the reaction mixture were completely homogenized. In each case, the degree of filling with

inorganic particles (i.e., the volume fraction of filler in mixture) did not exceed 20%. At the end of the syntheses, composite suspensions containing viscous polymer solutions and fillers were cast into polystyrene petri dishes with a diameter of 4 cm. Certain volumes of the mixtures were taken with a syringe to manufacture the composite fibers by electrospinning method. As water was removed from the structure by evaporation, the suspensions turned into hydrogels in the form of films and fibers. The labeling of the samples in accordance with the compounds used are shown in Table 1.

2.3. Electrospinning of filled PVA fibers

The study of capillary-free electroforming process of poly(vinyl alcohol) solutions and the fabrication of nano-/microscale non-woven samples based on composite suspensions PVA_1788/CC/H_2O, PVA_1788/CP/H_2O and PVA_1788/CC/CP/H_2O, were conducted using a laboratory unit "NANOSPIDER" NS LAB 200S (ELMARCO, Czech Republic). In order to obtain the fibers filled with particles in the calcium phosphate – calcium carbonate system, 1 g of each composite mixture was diluted with 0.1 g of water and placed on a cylindrical electrode located at the bottom of the electrospinning chamber. Due to the action of an electric field, the jets were drawn out of the suspensions distributed on the electrode in a thin layer, and stretched to diameters ranging from several microns down to several hundred nanometers. The jets hardened by water evaporation were then deposited on the fabric substrate of the upper electrode. The working distance between the forming and collecting electrodes was 16 cm, and the maximum voltage used during the process was limited to 45 kV.

2.4. Characterization

2.4.1. Viscosity measurements

The viscosity of partially hydrolyzed poly(vinyl alcohol) solutions of various molecular weight was studied using two viscometer types.

A capillary Ubbelohde viscometer (Fungilab, Spain) was used to determine reduced and intrinsic viscosities of diluted polymer solutions by measuring the time of leakage through the capillary with a diameter of 5.6 mm. A series of experiments was carried out on the basis of the initial 1% polymer solutions when thermostating in a water-bath system at a temperature of 25 °C.

The dynamic viscosity of poly(vinyl alcohol) solutions in a wide concentration range was studied using sinusoidal vibration viscometer SV-10 (A&D Company Ltd., Japan) equipped with low-frequency sensor plates (30 Hz). The operating measurement range of the device was 0.3–10000 mPa·s.

2.4.2. Phase composition

Phase composition of the obtained hydrogels was investigated on the basis of film samples (1 cm × 1 cm) by x-ray diffraction method (XRD) (Cu Ka radiation, 2θ 2–70°, diffractometer with rotating anode Rigaku D/Max-2500, Japan). Qualitative analysis of the phases was performed using ICDD PDF2 database.

Table 1
Labeling of the samples obtained in the form of films and fibers.

Polymer type	Labeling of the fillers	Expected phase compositions of the fillers	Labeling of composite hydrogels
PVA_1788	CC	$CaCO_3$ – calcite, vaterite	PVA_1788/CC/H_2O
	CP	$CaHPO_4{\cdot}2H_2O$, $Ca_{10}(PO_4)_6(OH)_2$	PVA_1788/CP/H_2O
	CC/CP	$CaCO_3$ – calcite, vaterite, $CaHPO_4{\cdot}2H_2O$, $Ca_{10}(PO_4)_6(OH)_2$	PVA_1788/CC/CP/H_2O

2.4.3. Microstructure

The microstructure of filler particles in composite films was studied by means of scanning electron microscopy (SEM) using thermal-emission microscope Carl Zeiss NVision 40 (Carl Zeiss, Germany) in the secondary electron mode (InLens detector). Before conducting the survey of the samples, a carbon layer was sprayed on the films under study to ensure their conductivity.

Fiber formation ability of composite suspensions based on poly(vinyl alcohol) at a given degree of filling with particles in the calcium phosphate – calcium carbonate system, as well as the structure of the obtained samples were shown by atomic force microscopy data (Ntegra Prima microscope, Russia). The measurements were performed in semi-contact mode using a probe sensor CSG01 (size 3.4 × 1.6 × 0.3 mm, needle tip radius 10 nm, rigidity 0.03 N/m).

2.4.4. Thermal analysis

The behavior of composite samples during the heat treatment in the temperature range of 25–1000 °C at a heating rate of 10 °C/min was described by thermal analysis (TG – thermogravimetry, DTA – differential thermal analysis) with mass spectrometric detection using thermal analyzer Netzsch STA-409 PC Luxx (Germany) equipped with quadrupole mass spectrometer QMS 403C Aëolos (Germany).

2.4.5. Cytotoxicity assessment

In vitro study of cytotoxicity was carried out on the basis of extracts from composite films in accordance with ISO 10993.5-99 requirements. The DMEM/F-12 (1:1, "Life technologies", USA) culture medium supplemented with 100 units ml^{-1} of penicillin/streptomycin was used as a model medium for the preparation of extracts under aseptic conditions for 72 h at 37 °C. In each case, the extraction medium was added in an amount of 1 ml per 0.2 g of the sample.

In the course of the study, primary culture of stromal cells isolated from the rudiments of human third molars (DPSC) was used. Aseptically extracted tooth rudiments were crushed with scissors to the size of 1–2 mm^3 and dissociated by treatment in 0.25 % trypsin – 0.02 % EDTA solution (PanEco, Russia) for 30 min at 37 °C. The isolated cells were centrifuged for 3 min and then placed in the culture medium DMEM/F-12 with 10 % of EtSH and 2 mM of L-glutamine. The cell cultivation was conducted in CO_2-atmosphere at a temperature of 37 °C. As the cells grew and reached a subconfluent state, they were treated with trypsin-EDTA solution and passed into new vials. The cells on the fourth passage were applied for the research.

The cells were seeded into the wells of a tablet at a concentration of 50000 cells/cm^2 in DMEM/F-12 medium containing 5% FBS. After 18 h, the medium was replaced with 100 μl of tested extracts. A positive control was performed by adding dimethyl sulfoxide (DMSO) to the culture medium, and as a negative control, DMEM/F-12 medium kept for 72 h was added. Culture medium exposed to specified conditions and procedures was used as a background control.

The study of the extracts for cytotoxicity was performed using MTT-test based on the reduction of colorless tetrazolium salt (3-[4,5-dimethylthiazol-2-yl]-2,5-diphenyltetrazolium bromide, MTT) by mitochondrial and cytoplasmic dehydrogenases of living metabolically active cells, which led to the formation of formazane blue crystals soluble in DMSO. 24 h after applying the extracts, the culture medium was removed and 100 μl of MTT-solution (0.5 mg/ml) was added to each sample in a DMEM/F-12 medium without serum. After holding for 3 h in a humidified CO_2-atmosphere, the liquid in the system was replaced with DMSO solution, and the resulting formazane salts were dissolved by shaking the tablet at a room temperature. The amount of reduced formazane was determined by optical density of the solutions using photometer (680 model, BIO-RAD, USA) at a wavelength of 540 nm.

3. Results and discussion

In the framework of this study, three types of poly(vinyl alcohol)

solutions of various concentrations were examined for viscosity using two techniques. The viscometry data are presented in Fig. 1. Based on the Mark-Houwink equation $[\eta] = KM^a$ with the parameters taken from the literature ($a = 0.72$, $K = 8.86 \cdot 10^{-4}$) and the intrinsic viscosity [η] values determined by extrapolating the linear dependences $\eta_{reduced}(c)$ on the ordinate axis in a narrow concentration range (Fig. 1a), molecular weights of polymers were estimated (Table 2). Typical for poly(vinyl alcohol) solutions dynamic viscosity curves were obtained in the concentration range of 6–12 wt % (Fig. 1b). Specified concentrations were chosen on the basis of experimental data, according to which electrospinning can be performed without hindrance. The data shows that the viscosity values increase more sharply when switching from a low-molecular to a higher-molecular poly(vinyl alcohol), which is consistent with the nature of the studied polymer solutions. Thus, the viscosity measurement limit of the viscometer is violated for aqueous solution containing PVA_2488 at a concentration of 12 wt %, so that the value cannot be determined. According to the results of electrospinning carried out from the polymer solutions, the most stable fiber formation process in a given concentration range was observed for solutions containing poly(vinyl alcohol) with the intermediate mass and dynamic viscosity values (PVA_1788). In particular, the droplet surface deformation for

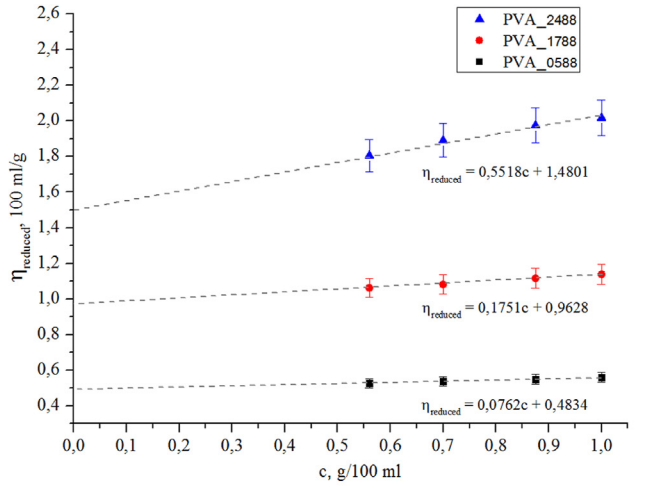

a

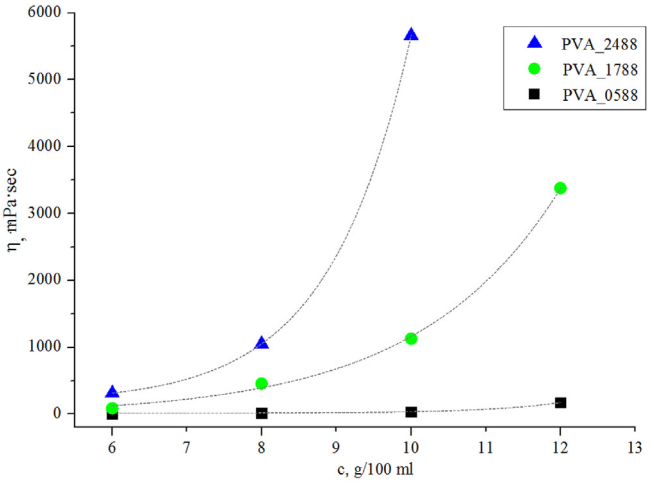

b

Fig. 1. Viscometry data for poly(vinyl alcohol) solutions of various molecular weights: the dependence of the reduced viscosity ($\eta_{reduced}$) on the concentration and its extrapolation on Y-axis **(a)**, dynamic viscosity curves in the concentration range of 6–12 wt % **(b)**.

Table 2
Properties of studied poly(vinyl alcohol) solutions.

Polymer type	[η], 100 ml/g	Molecular weight, kDa	c, wt %	Voltage of fiber formation, kV
PVA_0588	0.48	41.56	12	30
PVA_1788	0.96	124.07	8	27
PVA_2488	1.48	245.54	6	36

PVA_1788-based solution with the concentration of 8 wt %, was detected at a relatively low operating voltage of 21 kV, and layer-by-layer deposition of elastic fibers on the substrate occurred at 27 kV. The formation of fibers from the solutions of PVA_0588 is hindered due to the low surface tension of the droplet, which leads to its spreading over the electrode. However, at higher concentrations (>10–12 wt %), the tendency to form thin light fibers increases. In the case of PVA_2488-based solutions, the fiber manufacturing requires high operating voltages, and in contrast to the solutions of low-molecular poly(vinyl alcohol), unstable formation of nano-/microfibers take place at significantly low concentrations. The main characteristics of studied polymer solutions, including the intrinsic viscosity values, optimal concentrations for electrospinning and operating voltages of fiber formation, are reported in Table 2.

Samples of hydrogels in the form of films and fibers were obtained on the basis of PVA_1788 solutions and pre-synthesized CC-, CP- and CC/CP-powders. The fiber manufacturing by means of electrospinning was conducted in accordance with the parameters given in Table 3. Thus, the fiber formation was proved to occur from the prepared composite solutions with selected polymer concentration and degree of filling with powders. At the same time, the fibers were formed most easily in the case of PVA_1788/CC/CP/H_2O-sample, which confirms that CC/CP-filler possesses high uniformity of nanoscale components distribution.

It is widely known that PVA types of specified viscosity range that were used in this work, as well as relatively small degrees of filling with inorganic particles, lead to a significantly high degradation rate of polymer films and fibers in aqueous solutions. That fact was also confirmed by additional experiments, according to which partial degradation of composite strips with the mass of ~ 0.23 g and size of ~ 15 × 43 mm in 0.9 % aqueous NaCl solution occurs within 80 min. Thus, in its pure form (that is, without any crosslinking agents or another polymer component added to the hydrogel matrix) the use of PVA for medical purposes is difficult due to the partial dissolution of the materials and weak mechanical characteristics. However, it should be noted that the purpose of this work is precisely aimed at demonstration of possibility to fabricate fibrous and film objects with discussed filler compositions based on PVA matrices. In the future, the study can be expanded by introducing an additional component into the polymer component, using significantly high concentrations of polymer in order to obtain strong hydrogel structures, or increasing the degree of filling with particles. In the last two cases, the question of fiber fabrication should be reconsidered, since the use of electrospinning in these conditions occurs with hindrance due to a number of technological aspects. At this stage, the key objective was associated with the consideration of materials including the PVA matrix as model objects with compositions, biological compatibility and conditions for obtaining that can be further modified for use in regenerative approaches. Thus, the mechanical properties of

Table 3
Values of operating voltages during the fiber formation process on the basis of composite solutions.

Sample	Voltage of surface deformation, kV	Voltage of fiber formation, kV
PVA_1788/CC/H_2O	29	33
PVA_1788/CP/H_2O	31	42
PVA_1788/CC/CP/H_2O	26–27	28

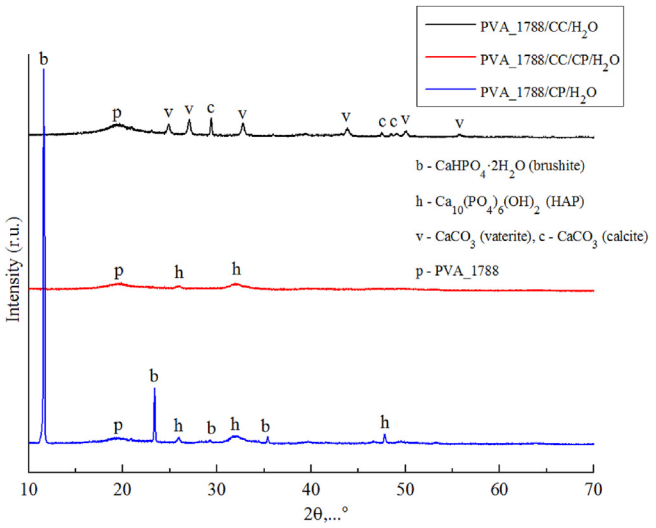

Fig. 2. XRD spectra of the composite films obtained from poly(vinyl alcohol) solutions (8 wt %) filled with pre-synthesized powders in the calcium phosphate – calcium carbonate system at a filling degree of 20 %. The identified phases are shown on the figure.

model objects, including the tensile and flexural strength, which are usually observed in the framework of such studies, fade into the background.

The XRD data for composite hydrogels PVA_1788/CC/H_2O, PVA_1788/CP/H_2O and PVA_1788/CC/CP/H_2O obtained in the form of films are shown in Fig. 2. Each of the diffractograms contains a diffuse maximum at $2\theta = 20^\circ$ that defines the poly(vinyl alcohol) crystal phase. The presence of this maximum is believed to characterize the diffraction on the crystal structure with an orthorhombic unit cell, in particular, on a system of crystal planes (101). According to Ref. [34], the maximum can be explained by the presence of a short-range order in the polymer chains arrangement. The diffractograms show that the insertion of fillers into the polymer films results in low intensity of the diffraction maximum, which is attributed to a decrease in the crystallinity degree of poly(vinyl alcohol). The phase compositions of fillers in films are consistent with those for pre-synthesized nanopowders [33]. Thus, the PVA_1788/C-C/H_2O hydrogel contains calcite and vaterite modifications, and the PVA_1788/CP/H_2O composite film includes hydroxyapatite and brushite phases. The exact composition of the x-ray amorphous CC/CP-filler obtained as a result of the synthesis from mixed-anionic solution containing HPO_4^{2-} and CO_3^{2-}-anions, cannot be identified directly due to the high uniformity of components distribution. However, the composition of CC/CP-powder can be assessed by heating the sample in the temperature

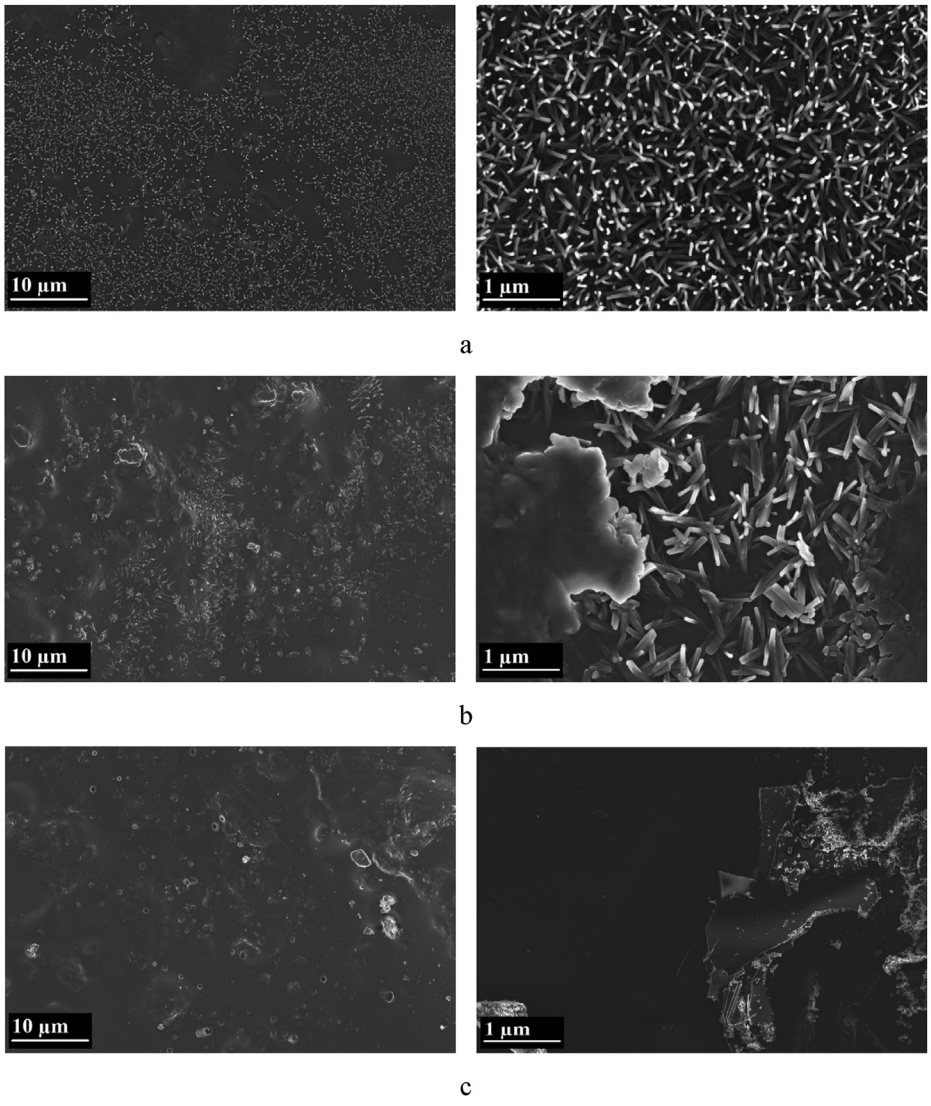

Fig. 3. SEM images of the composite films PVA_1788/CC/H_2O **(a)**, PVA_1788/CC/CP/H_2O **(b)** and PVA_1788/CP/H_2O **(c)** at various magnifications.

range of 600–800 °C. In the work [33], the authors assumed that the nanopowder synthesized under the same conditions contained $CaCO_3$--component that interacted with the initial brushite phase or its decomposition product calcium pyrophosphate ($Ca_2P_2O_7$) upon heating to form calcium orthophosphate $Ca_3(PO_4)_2$ (equation (4) – (5)).

$$2CaHPO_4 + CaCO_3 \rightarrow Ca_3(PO_4)_2\downarrow + CO_2\uparrow + H_2O \quad (4)$$

$$Ca_2P_2O_7 + CaCO_3 \rightarrow Ca_3(PO_4)_2\downarrow + CO_2\uparrow \quad (5)$$

The diffraction pattern of composite film PVA_1788/CC/CP/H_2O indicates the presence of hydroxyapatite phase low-intensity maxima. Presumably, the phase composition of CC/CP-filler in this sample can be defined by the reactions (1)–(3), according to which $CaCO_3$, $Ca_{10}(PO_4)_6(OH)_2$ and $CaHPO_4{\cdot}2H_2O$ were jointly precipitated from aqueous mixed-anionic solution.

For the obtained composite films, in contrast to pure poly(vinyl alcohol)-based films, a decrease in the transmission capacity can be observed visually. It should be noted that the sample containing CC/CP-filler possesses significant optical transparency, which confirms that intensive crystallization on the surface of the film does not take place due to simultaneous presence of HPO_4^{2-}/PO_4^{3-}- and CO_3^{2-}-anions.

The results of scanning electron microscopy for composite films are presented in Fig. 3. Morphological observations show that carbonate-containing samples (PVA_1788/CC/H_2O, PVA_1788/CC/CP/H_2O) are characterized by the presence of subparallel splices of elongated calcite crystals [35] with a single crystal average height of 430 nm and a thickness of 40 nm (Fig. 3a). The smooth surface of the agglomerates can be associated with the method of materials preparation from viscous polymer solutions [36]. According to micrographs, composite film PVA_1788/CP/H_2O includes the particles of a lamellar morphology with the lateral dimensions varying from 2 to 40 μm (Fig. 3c). It is known from the literature that the brushite precipitates crystallize mainly in the form of triangular platelets, sticks or wedge-shaped formations [37], and hydroxyapatite particles, depending on the synthesis conditions, can have spherical, acicular or lamellar shape [38]. Specified morphology type is hereby consistent with the phase composition of the filler represented by the mixture of brushite and hydroxyapatite phases. Additionally, phosphate particles embedded in hydrogels exhibit a defective structure, i.e. most of the platelets have fractures ranging in size from 2 to 30 μm. This moderately rough defective surface of the films is likely to provide favorable conditions for cell cultivation. The CC/CP-filler in the film PVA_1788/CC/CP/H_2O contains aggregated calcium phosphate platelets of a smaller size (up to 20 μm), which is explained by hindered crystallization on the surface of the film in the presence of carbonate anions.

Atomic force microscopy (AFM) micrographs of electrospun nonwoven materials based on poly(vinyl alcohol) and calcium salts are shown in Fig. 4. The morphological features of nanofibers can be identified on the basis of 2D- and 3D-images made in scan area 10 × 10 μm, 15 × 15 μm and 25 × 25 μm. Thus, the manufactured fibers have thickness varying from 195 nm to 523 nm. 2D-images show that composite fibers obtained from suspensions with inorganic fillers content of 20 % under specified electrospinning conditions contain sphere-like aggregates of particles with the largest detected diameter of 4.762 μm for PVA_1788/CC/CP/H_2O-sample (Fig. 4b). Reduced particle aggregation of the fillers in the viscous media of polymer solutions during hydrogels preparation results in high-contrast edges of aggregates on the micrographs. Despite the high uniformity of nanopowders distribution in polymer solutions, the AFM data demonstrates a relatively rough surface when compared to pure poly(vinyl alcohol) fibers described in the literature [39]. In a number of papers related to the development of polymer-based materials for cell cultivation it is reported that smooth surfaces are not adapted for cell attachment. Thus, the research [40] demonstrates the introduction of calcium phosphates (β-TCP) into chitosan matrix in order to improve the roughness of composite chitosan/β-TCP microspheres. In that case, the roughness measured by profilometers did not exceed 2 μm. AFM data for composite fibers investigated in the present work show roughness values of approximately 1.2–1.5 μm (Fig. 4c). According to Ref. [41], moderate surface roughness significantly increases cell attachment and promotes the generation of alkaline phosphatase activity and calcium nodule formation compared with the other groups. Since microscale surface roughness is known to have positive effect on both in vitro and in vivo cell proliferation due to enhanced adhesion of the cells [42], more detailed study on the surface parameters of the obtained fibrous materials could be the subject of further research.

The study of microscale roughness, which we expect will further promote cell proliferation, was shown using two types of microscopy, and at this stage of work, its effect on cell proliferation and differentiation is assumed but not proved precisely. The influence of roughness on cell behavior will be further supported by biological experiments on materials with a modified PVA matrix. Possible ways of modification were discussed earlier.

The thermal stability of the samples was studied on the basis of composite films and pure PVA_1788-based film. The results of TG and DTA analyses are presented in Fig. 5. According to DTA data, the thermal transformations of pure PVA_1788-based film occur in three main stages (Fig. 5a). The first stage in the temperature range of ~100–180 °C is accompanied by the absorbed water removal and partial polymer destruction, which leads to a mass loss of 5 %. At the second stage (~210–420 °C), the decomposition of poly(vinyl alcohol) continues with the formation of substantial CO_2 and H_2O amounts detected by mass spectrometer; endothermic peaks are observed at 224 °C, 287 °C and 402 °C, and the total mass loss reaches about 75 %. The final stage of polymer film decomposition includes its complete combustion at 600 °C; an endothermic peak is also observed at 491 °C. The presence of inorganic fillers in the films does not have a significant effect on the degradation process of polymer matrix. At the initial stage of thermal treatment, for phosphate-containing samples a slight decrease in mass (2–3 %) is observed due to the stepwise removal of crystallization water from brushite (Fig. 5c and d). PVA_1788/CC/H_2O-sample, as expected, undergoes a mass loss related to the carbonate decomposition (>700 °C) (Fig. 5b). Moreover, in the temperature range of 120–470 °C a decomposition of by-product CH_3COONH_4, as well as chemical reactions described in Ref. [33], may take place.

The study on cytotoxicity showed no toxic effect on the cells of the extracts from PVA_1788/CC/H_2O, PVA_1788/CP/H_2O and PVA_1788/CC/CP/H_2O samples. The DPSC metabolic activity data is shown in Fig. 6. A significant increase in optical density of the solutions, to which the extracts from PVA_1788/CC/H_2O and PVA_1788/CC/CP/H_2O films were added, may indicate the presence of water-soluble factors that stimulate the cell activity. According to the results, the reduced cell activity in the presence of extracts from composite film containing $CaHPO_4{\cdot}2H_2O$/$Ca_{10}(PO_4)_6(OH)_2$ phases probably takes place due to acidification of the medium caused by acid salt in the material. At the same time, the extracts of the sample containing CO_3^{2-}- and PO_4^{3-}/HPO_4^{2-}-anions have the highest cell activity index, which can be considered, to some extent, as the compensatory effect of simultaneous presence of CC-filler exhibiting a slight alkalinity, and the mixture of phosphates with the above mentioned phase composition. Statistical analysis of the results on DPSC metabolic activity conducted using the nonparametric Mann-Whitney *U* test did not show significant differences with the control when exposed to extracts from PVA_1788/CP/H_2O, which indicates the absence of water-soluble factors that have a toxic or stimulating effect on the primary cell culture isolated from the tooth pulp.

In the framework of the current research, the increased metabolic activity of the samples containing CO_3^{2-}-groups compared with the sample PVA_1788/CP/H_2O is presumably explained by the fact that the fibroblast growth factor bFGF is usually adsorbed and released into the external environment from the surface of the particles of CO_3^{2-}-containing samples in greater quantities than in samples based on calcium phosphates. This statement has been described quite well in the work [43] throughout the hydroxyapatite and carbonate substituted hydroxyapatite

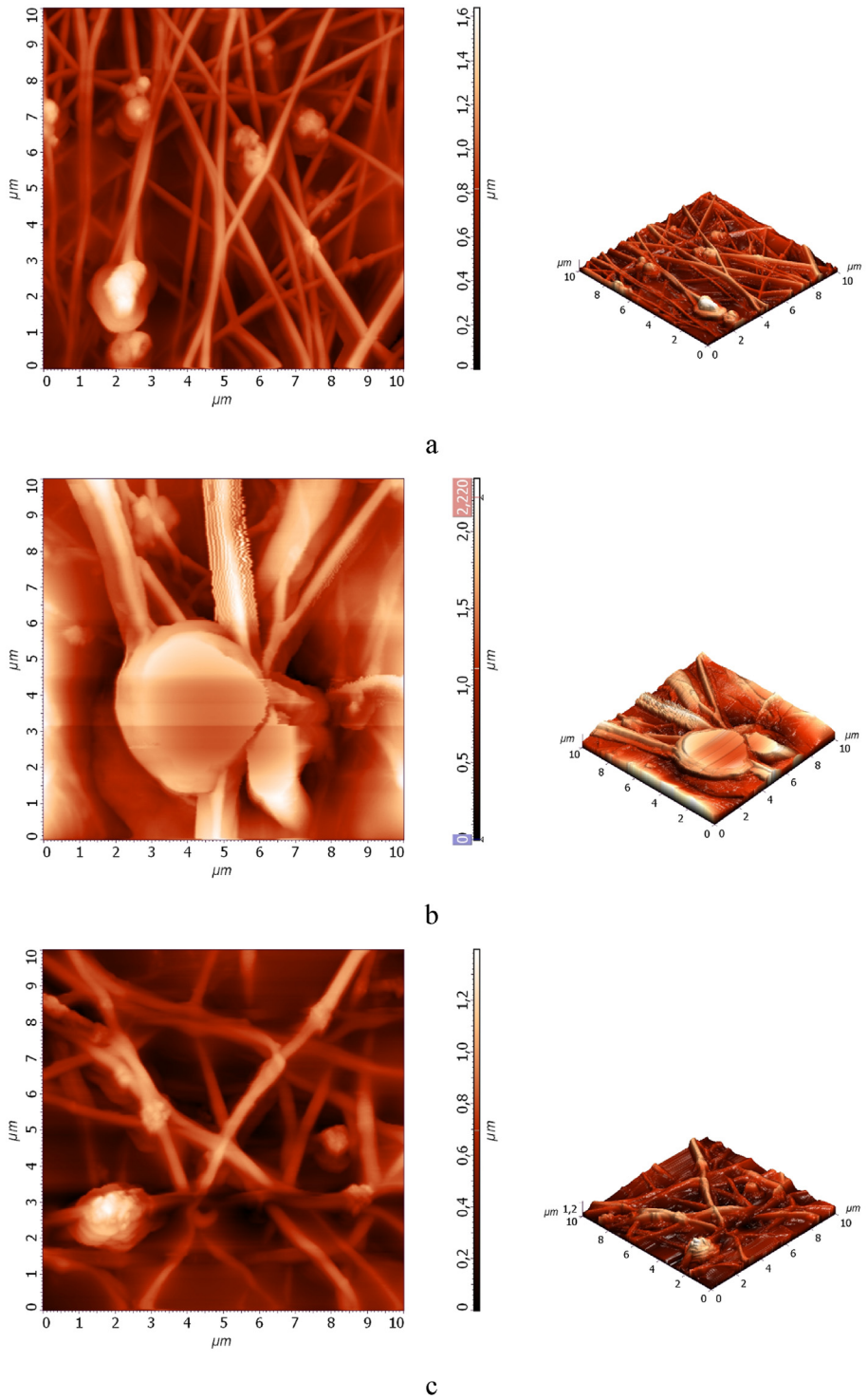

Fig. 4. 2D- (left) and 3D- (right) AFM images of the composite nanofibers PVA_1788/CC/H_2O **(a)**, PVA_1788/CC/CP/H_2O **(b)** and PVA_1788/CP/H_2O **(c)** manufactured by electrospinning.

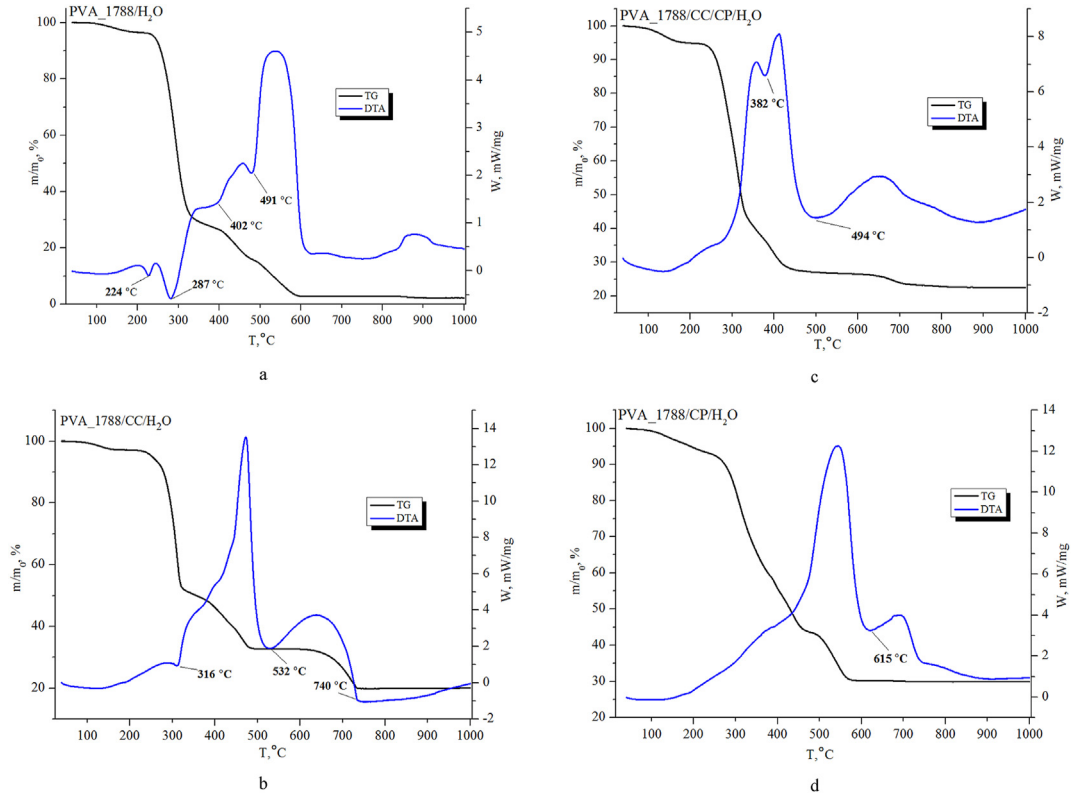

Fig. 5. TG and DTA data for pure PVA_1788-based film **(a)**, and composite films PVA_1788/CC/H_2O **(b)**, PVA_1788/CC/CP/H_2O **(c)**, PVA_1788/CP/H_2O **(d)**. The main endothermic peaks related to chemical transformations while heating are shown on the figures.

study of bioactivity. Apparently, this is due to the special topography and surface relief of the investigated fillers, the microscopy of which is presented above. Thus, the initial assumption regarding the positive effect of the carbonate ion on composite materials bioactivity put forward earlier was somehow justified.

During long-term incubation, which is usually carried out for 1, 3, 5 and 7 days, the effectiveness of cell differentiation cannot be established because the film materials quickly degrade in solutions and a day after the start of exposure, it is difficult to conduct a standard experiment. This problem can be eliminated in the course of further research and modification of the materials. The view of film composite samples after three days of exposure in the culture medium is shown in Fig. 7.

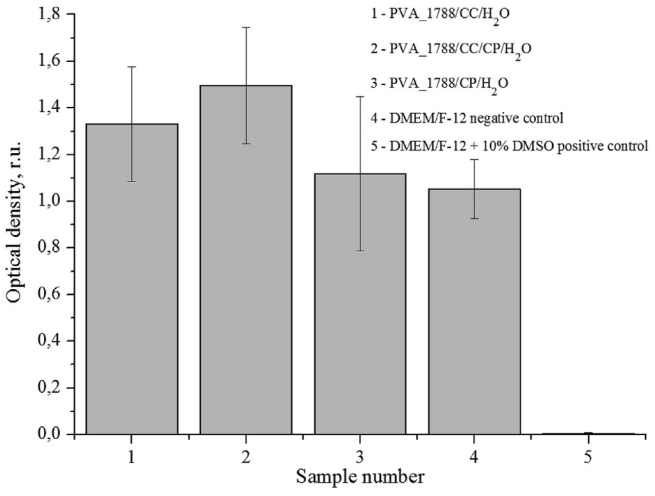

Fig. 6. Metabolic activity of dental pulp stem cells according to the results of MTT-test during incubation for 48 h with three-day extracts from the studied materials: 1 – PVA_1788/CC/H_2O film, 2 – PVA_1788/CC/CP/H_2O film, 3 – PVA_1788/CP/H_2O film, 4 – negative control (DMEM/F-12 medium), 5 – positive control (DMEM/F-12 + 10 % DMSO).

4. Conclusions

A method for obtaining new composite materials made up of poly(vinyl alcohol) hydrogels filled with calcium phosphate and/or calcium carbonate particles by combining viscous polymer solutions and presynthesized powders was proposed. Based on the selected parameters for the preparation of the initial composite suspensions, including polymer solution concentration (8 wt %) and particle filling degree (20 %), both films and fibers were manufactured without hindrance. Composite fibers obtained using the advanced electrospinning technology were shown to have a unique structure with fiber thickness distribution in the nanoscale range (~190–530 nm) and sphere-like defective aggregates of fillers. Moreover, the addition of CO_3^{2-}-anion into the sample containing PO_4^{3-}/HPO_4^{2-}-anions led to a significant simplification of fiber forming process resulted in lower operating voltages. Therefore, it can be concluded that the joint presence of specified anions prevents intensive crystallization of filler particles and makes it possible to obtain a new class of fibrous bioactive materials. The compositions of the materials represented by biocompatible calcium salts ($CaHPO_4{\cdot}2H_2O$, $Ca_{10}(PO_4)_6(OH)_2$, $CaCO_3$) and biosoluble poly(vinyl alcohol) phase, as well as microscale surface roughness promoting the cell proliferation and adhesion, let us consider the samples under study as prospective model materials for use in the field of regenerative medicine. The results of cytotoxicity study consistent with the structural investigation confirm the biological activity of the samples in the presence of dental pulp stem cells and reveal a wide range of possibilities for their further study as bioscaffolds.

Fig. 7. Degradation of film materials in cultivation solutions within 3 days: 1 – PVA_1788/CC/H_2O film, 2 – PVA_1788/CC/CP/H_2O film, 3 – PVA_1788/CP/H_2O film. The change in color of the samples reflects the change in pH (yellow color corresponds to more acidic environment, crimson color corresponds to moderately neutral environment).

CRediT authorship contribution statement

K. Kh Peranidze: Conceptualization, Investigation, Visualization. **T.V. Safronova:** Supervision, Data curation. **N.R. Kil'deeva:** Supervision. **M.V. Chernogortseva:** Investigation, Data curation. **I.I. Seleznева:** Investigation. **T.B. Shatalova:** Investigation. **J.V. Rau:** Editing.

Declaration of competing interest

The authors declare that they have no known competing financial interests or personal relationships that could have appeared to influence the work reported in this paper.

Acknowledgements

The present research work was supported by the Russian Foundation for Basic Research (grants No. 18-29-17059 and 18-29-11079). The equipment used in the study was purchased on the basis of funding of Moscow State University Development Program.

References

[1] B. Dhandayuthapani, Y. Yoshida, T. Maekawa, D.S. Kumar, Polymeric scaffolds in tissue engineering application: a review, Int. J. Polym. Sci. 2011 (2011) 1–19, https://doi.org/10.1155/2011/290602.
[2] R.E.B. Fitzsimmons, M.S. Mazurek, A. Soos, C.A. Simmons, Mesenchymal stromal/stem cells in regenerative medicine and tissue engineering, Stem Cell. Int. (2018) 1–17, https://doi.org/10.1155/2018/8031718, 2018.
[3] X. Ma, X. Zhang, Y. Jia, S. Zu, S. Han, D. Xiao, H. Sun, Y. Wang, Dexamethazone induces osteogenesis via regulation of hedgehog signalling molecules in rat mesenchymal stem cells, Int. Orthop. 37 (7) (2013) 1399–1404, https://doi.org/10.1007/s00264-013-1902-9.
[4] C.H. Chung, E.E. Golub, E. Forbes, T. Tokuoka, I.M. Shapiro, Mechanism of action of β-glycerophosphate on bone cell mineralization, Calcif. Tissue Int. 51 (4) (1992) 305–311, https://doi.org/10.1007/BF00334492.
[5] J. Michel, M. Penna, J. Kochen, H. Cheung, Recent advances in hydroxyapatite scaffolds containing mesenchymal stem cells, Stem Cell. Int. (2) (2015) 1–13, https://doi.org/10.1155/2015/305217, 2015.
[6] A.C.O. Carreira, W.F. Zambuzzi, M.C. Rossi, R.A. Filho, M.C. Sogayar, J.M. Granjeiro, Chapter ten – bone morphogenetic proteins: promising molecules for bone healing, bioengineering, and regenerative medicine, Vitam. Horm. 99 (2015) 293–322, https://doi.org/10.1016/bs.vh.2015.06.002.
[7] A.A. Tikhonov, E.V. Kukueva, P.V. Evdokimov, E.S. Klimashina, V.I. Putlyaev, I.M. Shcherbakov, V.E. Dubrov, Synthesis of substituted octacalcium phosphate for filling composite implants based on polymer hydrogels produced by stereolithographic 3D printing, Inorg. Mater. 54 (10) (2018) 1062–1070, https://doi.org/10.1134/S0020168518100175.
[8] S.T. Bendtsen, S.P. Quinnell, M. Wei, Development of a novel alginate – polyvinyl alcohol – hydroxyapatite hydrogel for 3D bioprinting bone tissue engineered scaffolds, J. Biomed. Mater. Res. A 105 (5) (2017) 1457–1468, https://doi.org/10.1002/jbm.a.36036.
[9] M. Filippi, G. Born, M. Chaaban, A. Scherberich, Natural polymeric scaffolds in bone regeneration, Front. Bioeng. Biotechnol. 8 (2020) 474–502, https://doi.org/10.3389/fbioe.2020.00474.
[10] D.M. Zuev, E.S. Klimashina, P.V. Evdokimov, YaYu Filippov, V.I. Putlyaev, Preparation of β-$Ca_3(PO_4)_2$/poly(D,L-lactide) and β-$Ca_3(PO_4)_2$/poly(ε-caprolactone) biocomposite implants for bone substitution, Inorg. Mater. 54 (1) (2018) 87–95, https://doi.org/10.1134/S002016851801017X.
[11] N. Zhang, Y. Wang, W. Xu, Y. Hu, J. Ding, Poly(lactide-co-glycolide)/hydroxyapatite porous scaffold with microchannels for bone regeneration, Polymers 8 (6) (2016) 218–229, https://doi.org/10.3390/polym8060218.
[12] P. Chocholata, V. Kulda, V. Babuska, Fabrication of scaffolds for bone tissue regeneration, Materials 12 (4) (2019), https://doi.org/10.3390/ma12040568, 568–593.
[13] N. Alexandre, J. Ribeiro, A. Gartner, T. Pereira, et al., Biocompatibility and hemocompatibility of poilyvinyl alcohol hydrogel used for vascular grafting – in vitro and in vivo studies, J. Biomed. Mater. Res. A 102 (12) (2014) 4262–4275, https://doi.org/10.1002/jbm.a.35098.
[14] T.S. Gaaz, A.B. Sulong, M.N. Akhtar, A.A.H. Kadhum, A.B. Mohamad, A.A. Al-Amiery, Properties and applications of polyvinyl alcohol, halloysite nanotubes and their nanocomposites, Molecules 20 (12) (2015) 22833–22847, https://doi.org/10.3390/molecules201219884.
[15] L.S. Casey, L.D. Wilson, Investigation of chitosan-PVA composite films and their adsorption properties, J. Geosci. Environ. Protect. 3 (2) (2015) 78–84, https://doi.org/10.4236/gep.2015.32013.
[16] Y. Zhang, X. Huang, B. Duan, L. Wu, S. Li, X. Yuan, Preparation of electrospun chitosan/poly(vinyl alcohol) membranes, Colloid Polym. Sci. 285 (8) (2007) 855–863, https://doi.org/10.1007/s00396-006-1630-4.
[17] G. Michailidou, N.M. Ainali, E. Xanthopoulou, S. Nanaki, N. Kostoglou, E.N. Koukaras, D.N. Bikiaris, Effect of poly(vinyl alcohol) on nanoencapsulation of budesonide in chitosan nanoparticles via ionic gelation and its improved bioavailability, Polymers 12 (5) (2020) 1101–1123, https://doi.org/10.3390/polym12051101.
[18] W. Chang, X. Mu, X. Zhu, G. Ma, C. Li, F. Hu, J. Nie, Biomimetic composite scaffolds based mineralization of hydroxyapatite on electrospun calcium-containing poly(vinyl alcohol) nanofibers, Mater. Sci. Eng. C 33 (7) (2013) 4369–4376, https://doi.org/10.1016/j.msec.2013.06.023.
[19] S. Kissling, M. Seidenstuecker, I.H. Pilz, N.P. Suedkamp, H.O. Mayr, A. Bernstein, Sustained release of rhBMP-2 from microporous tricalciumphosphate using hydrogels as a carrier, BMC Biotechnol. 16 (1) (2016) 44–53, https://doi.org/10.1186/s12896-016-0275-8.

[20] S. Nkhwa, L. Iskandar, N. Gurav, S. Deb, Combinatorial design of calcium meta phosphate poly(vinyl alcohol) bone-like biocomposites, J. Mater. Sci. Mater. Med. 29 (8) (2018) 128–144, https://doi.org/10.1007/s10856-018-6133-6.
[21] M. Okamoto, B. John, Synthetic biopolymer nanocomposites for tissue engineering scaffolds, Prog. Polym. Sci. 38 (10–11) (2013) 1487–1503, https://doi.org/10.1016/j.progpolymsci.2013.06.001.
[22] M. Šupová, Substituted hydroxyapatites for biomedical applications: a review, Ceram. Int. 41 (8) (2015) 9203–9231, https://doi.org/10.1016/j.ceramint.2015.03.316.
[23] G. Spence, N. Patel, R. Brooks, N. Rushton, Carbonate substituted hydroxyapatite: resorption by osteoclasts modifies the osteoblastic response, J. Biomed. Mater. Res. A 90 (1) (2009) 217–224, https://doi.org/10.1002/jbm.a.32083.
[24] L.F. Koroleva, M.N. Dobrinskaya, I.S. Kamantsev, Doped calcium carbonate-phosphate used for bone tissue technology, Integr. Clin. Med. 1 (2) (2017) 1–7, https://doi.org/10.15761/ICM.1000108.
[25] S. Rokidi, C. Combes, P.G. Koutsoukos, The calcium phosphate – calcium carbonate system: growth of octacalcium phosphate on calcium carbonate, Cryst. Growth Des. 11 (5) (2011) 1683–1688, https://doi.org/10.1021/cg101602a.
[26] L.F. Koroleva, Nanocrystalline doped calcium carbonate-phosphates as a biomaterial for osteogenesis, Res. J. Pharmaceut. Biol. Chem. Sci. 5 (6) (2014) 704–710. ISSN: 0975-8585.
[27] A. Eltom, G. Zhong, A. Muhammad, Scaffold techniques and designs in tissue engineering functions and purposes: a review, Ann. Mater. Sci. Eng. 4 (2019) 1–13, https://doi.org/10.1155/2019/3429527, 2019.
[28] K.C. Gupta, A. Haider, Y. Choi, I. Kang, Nanofibrous scaffolds in biomedical applications, Biomater. Res. 18 (5) (2014) 1–11, https://doi.org/10.1186/2055-7124-18-5.
[29] J.P. Kennedy, S.P. McCandless, R.A. Lasher, R.W. Hitchcock, The mechanically enhanced phase separation of sprayed polyurethane scaffolds and their effect on the alignment of fibroblasts, Biomaterials 31 (6) (2010) 1126–1132, https://doi.org/10.1016/j.biomaterials.2009.10.024.
[30] G. Turnbull, J. Clarke, F. Picard, P. Riches, L. Jia, F. Han, B. Li, W. Shu, 3D bioactive composite scaffolds for bone tissue engineering, Bioact. Mater. 3 (3) (2018) 278–314, https://doi.org/10.1016/j.bioactmat.2017.10.001.
[31] C. Wang, W. Huang, Y. Zhou, L. He, et al., 3D printing of bone tissue engineering scaffolds, Bioact. Mater. 5 (1) (2020) 82–91, https://doi.org/10.1016/j.bioactmat.2020.01.004.
[32] D.G. Tamay, T.D. Usal, A.S. Alagoz, D. Yucel, N. Nasirci, V. Hasirci, 3D and 4D printing of polymers for tissue engineering applications, Front. Bioeng. Biotechnol. 7 (2019) 164–186, https://doi.org/10.3389/fbioe.2019.00164.
[33] T.V. Safronova, V.I. Putlyaev, YaYu Filippov, A.V. Knot'ko, E.S. Klimashina, K.Kh Peranidze, P.V. Evdokimov, S.A. Vladimirova, Powders synthesized from calcium acetate and mixed-anionic solutions, containing orthophosphate and carbonate ions, for obtaining bioceramics, Glass Ceram. 75 (3–4) (2018) 118–123, https://doi.org/10.1007/s10717-018-0040-7.
[34] S. Gaidukov, I. Danilenko, G. Gaidukova, Characterization of strong and crystalline polyvinyl alcohol/montmorillonite films prepared by layer-by-layer deposition method, Int. J. Polym. Sci. (2015) 1–8, https://doi.org/10.1155/2015/123469, 2015.
[35] K.T. Moreland, M. Hong, W. Lu, C.W. Rowley, D.M. Ornitz, J.J. De Yoreo, R. Thalmann, In vitro calcite crystal morphology is modulated by otoconial proteins otolin-1 and otoconin-90, PloS One 9 (4) (2014) 95333–95341, https://doi.org/10.1371/journal.pone.0095333.
[36] C. Kosanović, S. Fermani, G. Falini, D. Kralj, Crystallization of calcium carbonate in alginate and xanthan hydrogels, Crystals 7 (12) (2017) 355–370, https://doi.org/10.3390/cryst7120355.
[37] T.V. Safronova, V.I. Putlyaev, YaYu Filippov, T.B. Shatalova, D.S. Fatin, Ceramics based on brushite powder synthesized from calcium nitrate and disodium and dipotassium hydrogen phosphates, Inorg. Mater. 54 (2) (2018) 210–220, https://doi.org/10.1134/S0020168518020127.
[38] A.V. Kuznetsov, A.S. Fomin, A.G. Veresov, V.I. Putlyaev, I.V. Fadeeva, S.M. Bariov, Hydroxyapatite of platelet morphology synthesized by ultrasonic precipitation from solution, Russ. J. Inorg. Chem. 53 (1) (2009) 1–5, https://doi.org/10.1134/S0036023608010014.
[39] K. Sasipriya, R. Suriyaprabha, P. Prabu, V. Rajendran, Synthesis and characterization of polymeric nanofibers poly (vinyl alcohol) and poly (vinyl alcohol)/silica using indigenous electrospinning set up, Mat. Res. 16 (4) (2013) 824–830, https://doi.org/10.1590/S1516-14392013005000050.
[40] Q. Zan, C. Weng, L. Dong, P. Cheng, J. Tian, Effect of surface roughness of chitosan-based microspheres on cell adhesion, Appl. Surf. Sci. 255 (2) (2008) 401–403, https://doi.org/10.1016/j.apsusc.2008.06.074.
[41] Y. Deng, X. Liu, A. Xu, L. Wang, Z. Luo, Y. Zheng, F. Deng, J. Wei, Z. Tang, S. Wei, Effect of surface roughness on osteogenesis in vitro and osseointegration in vivo of carbon fiber-reinforced polyetheretherketone – nanohydroxyapatite composite, Int. J. Nanomed. 10 (1) (2015) 1425–1447, https://doi.org/10.2147/IJN.S75557.
[42] A.R. Jo, M.W. Hong, Y.S. Cho, K.M. Song, J.H. Lee, D. Sohn, Y.Y. Kim, Y.S. Cho, Assessment of cell proliferation in knitting scaffolds with respect to pore-size heterogeneity, surface wettability, and surface roughness, J. Appl. Polym. Sci. 132 (38) (2015) 42566–42573, https://doi.org/10.1002/app.42566.
[43] V. Midy, et al., Basic fibroblast growth factor adsorption and release properties of calcium phosphate, J. Biomed. Mater. Res. 41 (3) (1998) 405–411, https://doi.org/10.1002/(sici)1097-4636(19980905)41:3<405::aid-jbm10>3.0.co;2-h.